

REVIEW

**Open-framework aluminophosphates: synthesis,
characterization and transition metal modifications**

NEVENKA RAJIĆ

*Faculty of Technology and Metallurgy, Karnegijeva 4, 11000 Belgrade, Serbia and Montenegro
(e-mail: nena@tmf.bg.ac.yu)*

(Received 11 November 2004)

Abstract: This review is a brief summary of open-framework aluminophosphates and their transition metal-substituted modifications. The materials exhibit structural and compositional diversity, as well as a wide range of pore openings, which are crystallographically ordered and can be tuned by an appropriate choice of synthesis conditions. The diameters of the apertures, cages and channels fall in the range of 0.4 to about 1.5 nm, which recommends aluminophosphates for a novel area of application – nanocatalysis. Isomorphous substitution of the framework elements by transition metal ions which possess redox ability creates active sites inside the aluminophosphate lattice and opens routes towards shape selective bi-functional catalysis. In order to obtain an insight into the location of the transition metal ions, different characterization techniques have to be used.

Keywords: molecular sieves, catalysis, aluminophosphate, hydrothermal synthesis, open-frameworks.

CONTENTS

1. Introduction
2. Synthesis
 - 2.1. The role of the structure-directing agent
 - 2.2. The role of fluoride ions
 - 2.3. Crystallization using microwave hydrothermal processing
3. Isomorphous substitution in the aluminophosphates – MAPO and MAPSO sieves
 - 3.1. Titanium
 - 3.2. Vanadium
 - 3.3. Chromium
 - 3.4. Manganese
 - 3.5. Iron
 - 3.6. Cobalt
 - 3.7. Nickel
 - 3.8. Zinc
4. Conclusion

1. INTRODUCTION

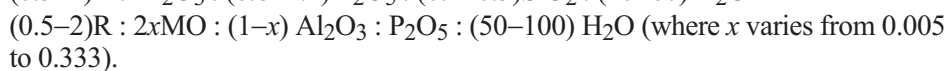
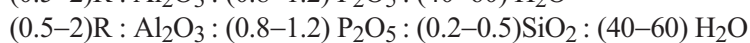
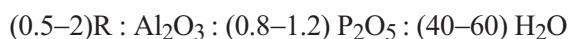
At the onset of the 1980's, the Union Carbide Laboratories reported a new family of molecular sieves based on aluminophosphates.^{1,2} The aluminophosphate molecular sieves, known as $\text{AlPO}_4\text{-}n$ (n refers to a distinct structure type), are built of strictly alternating AlO_4 and PO_4 tetrahedra. Their general formula can be expressed as $[(\text{AlO}_2)_x(\text{PO}_2)_x] \cdot y\text{H}_2\text{O}$ indicating that, unlike most zeolites, the aluminophosphate molecular sieves are ordered with an Al/P ratio that is always unity. However, in spite of this, aluminophosphate molecular sieves exhibit enhanced structural diversity. Among the more than 40 structures of $\text{AlPO}_4\text{-}n$, some are zeolite analogues but there are also novel, unique structures.³ Apart from their structural similarity, the crystal chemistry of AlPO_4 molecular sieves and zeolites differs considerably. Firstly, the aluminophosphate framework is neutral in contrast to the negatively charged aluminosilicate one. Secondly, the aluminium atoms in the aluminosilicate framework are always tetrahedrally coordinated as compared to the four, five or six coordinated aluminum atoms present in the aluminophosphate framework. These facts just serve as illustrations of the structural diversity of AlPO_4 molecular sieves.

The aluminophosphate molecular sieves exhibit not only structural but also compositional diversity. The porous aluminophosphate frameworks can be modified by other elements. Thus, the incorporation of silicon results in silicoaluminophosphate molecular sieves, $\text{SAPO-}n$.^{4,5} The addition of metal cations (M) yields porous metaloaluminophosphate, $\text{MAPO-}n$ ^{6,7} or metalosilicoaluminophosphates, $\text{MAPSO-}n$.⁸⁻¹² In the SAPO materials, silicon substitutes for phosphorus or for an aluminum-phosphorus pair, whereas the M cations substitute almost exclusively for aluminum. The MAPO and MAPSO materials encompass the characteristics of both zeolites and aluminophosphates, which results in their unique catalytic, ion-exchange and adsorbent properties.

2. SYNTHESIS

Aluminophosphate-based molecular sieves can be synthesized hydrothermally at 100–250 °C. Generally, AlPO_4 and SAPO crystallize at higher temperatures than the MAPO materials. However, apart from the temperature and time, the type of structure formed depends on the control of a number of variables, including the reactant gel composition, the individual characteristics of reactants, the type of template, pH, *etc.* Most of these variables are not independent and influence one another during the crystallization process. As an example, two different crystal structures¹³ can simultaneously crystallize from one in the same reaction mixture (their chemical formulas differing only in the water content). Moreover, CoAPSO-14 and CoAPSO-34 (the crystal type 14 being a novel one, whereas the 34 is analogous to the zeolite chabazite) crystallize also from the reaction mixture with the same mole ratio of reactants.¹⁴ However, whereas CoAPSO predominantly forms at 125 °C, CoAPSO is the main crystalline

phase at 160°C. Typically, the synthesis of AlPO_4 involves the use of an aqueous reaction mixture containing an aluminum source, a phosphate source and an amine and/or a quaternary ammonium salt. The aluminum source is usually aluminum isopropoxide or pseudo-boehmite, whereas orthophosphoric acid is most frequently the source of the phosphorus component. In the synthesis of SAPO, MAPO and MAPSO, silica sol and/or a solution of the M salt (usually acetate or sulphate) are introduced into the reactive mixture. Typical reaction mixtures have molar compositions as follows (R is an amine and/or a quaternary ammonium salt):



Despite the great efforts being made, the principles governing the formation of a porous crystalline materials are not yet well understood because of the complexity of hydrothermal crystallizations. Namely, hydrothermal crystallization occurs in a closed vessel where many chemical processes, interactions and equilibriums take place and change with time.¹⁵ Therefore, some novel *in situ* techniques, such as synchrotron X-ray powder diffraction or *in situ* solid state NMR, may contribute to a better understanding of the crystallization process.^{16,17}

Recently, it was found that crystallization of most aluminophosphates presumably involves a chain to layer transformation process, whereby the chains are ini-

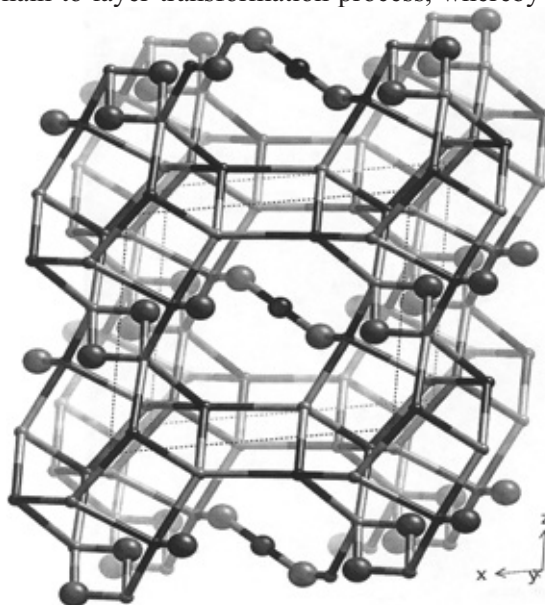


Fig. 1. The disrupted chabazite framework of $\text{AlPO}_4\text{-34}$. The Ni(II) complex is in the middle of the chabazite cage forming an unique P–O–Ni–O–P bridge. The disruption completely disappears on calcination.

tially hydrolyzed in solution, leading to the formation of other types of chain structures.^{18,19} The chains are built up of low-membered (4-MRS)Al₂P₂ rings (corner-sharing or edge-sharing). Condition of the chains leads to crosslinking and then to the formation porous layers and, subsequently, open-framework structures.^{19,20} Interestingly, investigations of open-framework zinc phosphates have led to a similar conclusion, *i.e.*, that the formation of the complex 3-D architecture may involve a process whereby chains and zero-dimensional monomers consisting of 4-MRs transform to a higher dimensional structure.^{21,22}

2.1. The role of the structure-directing agent

Organic amines or quaternary ammonium salts exhibit a critical structure-directing role in the synthesis of aluminophosphate-based molecular sieves. They exert both a steric and an electronic influence.²³ In their absence, no crystalline porous aluminophosphates form. More than eighty amines and quaternary ammonium salts have been used as template species. Their structure-directing specificity varies widely. For example, more than twenty templates lead to the formation of AlPO₄-5, which is the structure type with a nearly circular channel system having a diameter of 0.73 nm. On the other hand, several organic amines are known to produce different framework structures by slightly changing the synthesis variables. Thus, di-*n*-propylamine can be used in the synthesis of many aluminophosphate-based molecular sieves – AlPO₄-11, VPI-5, MAPO-39, CoAPO-43, CoAPO-50, SAPO-*n* (*n* = 5, 11, 31).^{24,25}

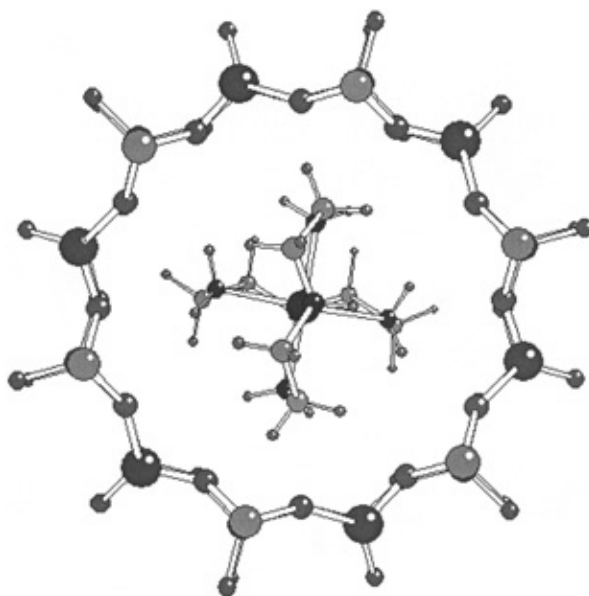


Fig. 2. [Ni(*ten*)₂]²⁺ ion inside a channel of AlPO₄-5 viewed down the channel's axis.

Recently, it was found that transition metal complexes may also act as structure-directing agents. Bis(cyclopentadienyl)cobalt(III) ions lead to the formation of both

channel-and cage-type molecular sieves, such as $\text{AlPO}_4\text{-5}$ and SAPO-16 .^{26,27} The bis(1,2-diaminoethane)dihydroxoNi(II) complex also exhibits a critical structure-directing role in the crystallization of $\text{AlPO}_4\text{-34}$.^{28,29} The as-synthesized material has a deformed (disrupted) chabazite structure with the Ni(II) complex being an integral part of the framework (Fig. 1). The complex forms an unusual P–O–Ni–O–P bridge across the chabazite cage, causing a disruption of the P–O–Al connectivity. The Al atoms associated with this disruption form double Al–OH–Al bridges and are 5-coordinated. However, despite the distortion of the chabazite-like framework, all of the P atoms and two of the three Al atoms in the asymmetric unit are in regular tetrahedral environments.

Also, the bis(bis-(2-aminoethyl)amine)nickel(II) complex ($[\text{Ni}(\text{ten})_2]^{2+}$ ion) plays a structure-directing role in the crystallization of $\text{AlPO}_4\text{-5}$.³⁰ Geometry considerations suggest that the $[\text{Ni}(\text{ten})_2]^{2+}$ ion almost exactly fits the channel dimensions and is held inside the channel by Van der Waals forces (Fig. 2).

In some cases, a partial decomposition, of the template species occurs under hydrothermal conditions and more than one species exerts a structure-directing role. Usually, organic amines decompose to ammonia. Thus, 1,2-diaminopropane partially decomposes during hydrothermal synthesis and both NH_4^+ and the doubly protonated diamine have a templating role.³¹ Also, it has been found that the ammonium ions resulting from the complete decomposition of a template (such as hexamethylenetetramine) can solely play a structure-directing role in the crystallization of $\text{AlPO}_4\text{-15}$ and CoAPO-15 .³²

The template species remain occluded in the as-synthesized products and it is necessary to remove them in order to make the aluminophosphate framework porous for further use. This can be achieved thermally by calcination in air or oxygen, usually at 400–600 °C. It has been found that the temperature at which the template removal occurs depends on the incorporated metal.³³ Calcination may sometimes be accompanied by a transformation of one crystalline phase into another. A typical example is the transformation of $\text{AlPO}_4\text{-21}$ to $\text{AlPO}_4\text{-25}$.^{34,35} In some cases the calcined product, such as $\text{AlPO}_4\text{-34}$, is thermally stable up to 1000 °C.^{36,37}

2.2. The role of fluoride ions

Crystallization of some open-framework aluminophosphates requires the presence of fluoride ions in the reaction mixture. It has been found that fluoride ions exhibit several roles: 1) they solubilize aluminum in the reaction mixture leading to a slower nucleation, thus rendering the formation of dense aluminophosphate phases less favorable, 2) they lead to slower crystal growth rates yielding crystals of larger size with fewer defects, and 3) the fluoride ions impart a structure-directing and templating effect by interacting with the framework.³⁸ In this last role, fluoride ions behave as bidentate ligands linking two aluminum ions (Fig. 3). Consequently, the aluminophosphate framework requires a cation to balance the charge. Generally, a protonated organic amine is the counter ion.

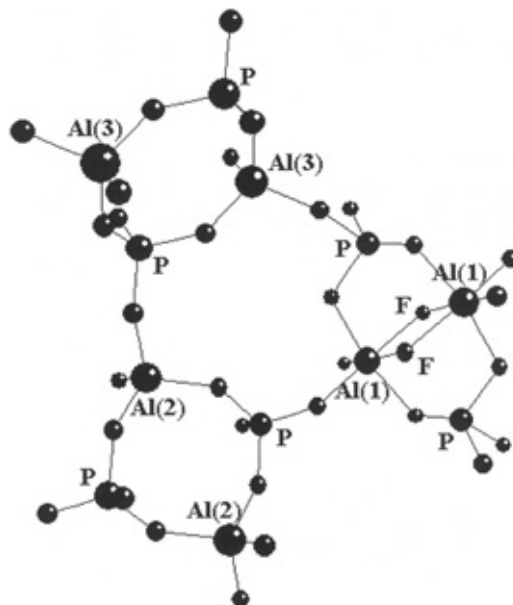


Fig. 3. Fluoride bridges in as-synthesized $\text{AlPO}_4\text{-34}$. The fluoride ions increase the coordination number of Al(1) atoms from 4 to 6.

The chabazite-like $\text{AlPO}_4\text{-34}$ has only been obtained from a fluoride-containing reaction medium. In the as-synthesized framework the fluoride ions interact with the lattice (Fig. 3) causing its deformation,^{37,38} the fluoride ions being completely removable by calcination.

2.3. Crystallization using microwave hydrothermal processing

A new technique combining hydrothermal and microwave heating can be employed for the preparation of aluminophosphates.^{39–44} The application of this technique reduces the crystallization time from a few days to a few minutes. As in illustration, the crystallizations of $\text{MnAPO-}n$ and $\text{MnAPSO-}n$ ($n = 5, 44$) are completed in 30 minutes.⁴⁰ Likewise, the formation of the first large $\text{AlPO}_4\text{-5}$ crystals is observed after only 60 s.⁴⁴ It is assumed that the microwaves destroy the hydrogen bridges between water molecules causing fast gel dissolution and the formation of Al–O–P building blocks. The gel contains self-assembled micro-arrays, which transform directly into the $\text{AlPO}_4\text{-5}$ structure.

3. ISOMORPHOUS SUBSTITUTION IN THE ALUMINOPHOSPHATES – MAPO AND MAPSO SIEVES

The substitution of Al by divalent metal ions generates Brønsted acid sites (acidic bridging OH groups) as well as Lewis acid sites (anionic vacancies deriving from missing lattice oxygens) in the aluminophosphate lattice. Incorporation of a transition metal cation, which can easily change its oxidation number also creates a

redox active site. The coupling of acidic with redox properties opens up routes towards shape selective bi-functional catalysis and to the design of novel catalysts. Clearly, knowledge of the location and the local structure (metal ion environment) of the incorporated metal ions is necessary for optimization and control of the catalytic activity in these systems.

Isomorphous substitution, *i.e.*, the replacement of Al^{3+} and/or P^{5+} by a tetrahedrally coordinated metal ion has been reported for more than 17 elements.^{45,46} Different characterization techniques are used in order to gain an insight into the location of the transition metal ions in an aluminophosphate framework. Generally, data on the location of the cations are collected with difficulty since the metal concentration is usually low. It is necessary to use more than one method if a reliable conclusion is to be reached (*i.e.*, the simultaneous application of several physical techniques is recommended). The following characterization methods are commonly applied: diffuse reflectance UV-Vis spectroscopy (DRS), electron spin resonance (ESR), electron spin echo modulation (ESEM), infrared (IR) and diffuse reflectance infrared Fourier transform (DRIFT) spectroscopies. Nuclear magnetic resonance spectroscopy (NMR), Mössbauer spectroscopy, X-ray absorption near-edge structure (XANES) and extended X-ray absorption spectroscopy for fine structure (EXAFS) are also employed occasionally.

A brief review on the characterization of the most commonly investigated metal ions incorporated into aluminophosphate-based molecular sieves is given in the ensuing text. All of these metals belong to the first transition series and are discussed here in the order of increasing atomic number.

3.1. Titanium

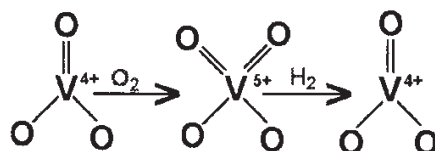
Tetrahedral titanium(IV) has been incorporated into several zeolites. These titanium-modified materials show remarkable catalytic activity in oxidation reactions using dilute aqueous hydrogen peroxide under mild conditions. The titanium-incorporated silicalite-1 (TS-1) has been one of the most relevant industrial catalyst in the last two decades. The catalytic activity is related to the tetrahedrally coordinated titanium incorporated in the framework.^{47–51} These facts have directed research to investigate the possibility of incorporation of titanium into the aluminophosphate framework. Incorporation of Ti(IV) has been studied by various methods. Thus, UV-Vis spectra of TAPSO-5 show a single relatively broad band between 200 and 310 nm, centered around 230 nm.⁵² The band is assigned to a charge transfer from oxygen atoms to the tetrahedral Ti^{4+} atoms. The absence of a band between 300–350 nm indicates that the anatase-like phase (the most common impurity in Ti-containing zeolites) is not formed during crystallization. Also, the appearance of Brønsted acid sites in the TAPO-5 and TAPO-36 confirms the insertion of titanium in the aluminophosphate lattice and supports the isomorphous substitution of titanium for phosphorus in these solids.⁵³

3.2. Vanadium

V_2O_5 -based catalysts have been widely used in industry for many catalytic processes, including oxidation reactions under mild conditions. Incorporation of metal ions exhibiting redox properties into an aluminophosphate framework with a well defined system of pores and cavities offers an opportunity for the preparation of novel oxidation catalysts. In this context, VAPO and VAPSO seem to be promising materials, whereas the incorporation of vanadium into tetrahedral aluminophosphate frameworks is still debatable (*vide infra*).

VAPO-5 and VAPSO-5 have been synthesized using tripropylamine (TPA) and hexamethylene-imine (HEM) as templates. A larger degree of incorporation of V takes place when HEM is used. Vanadium replaces both phosphorus and silicon. About three quarters of the vanadium in the samples are found to be present in tetrahedral coordination and the rest in square pyramidal or distorted octahedral coordination.⁵⁴ However, EPR spectra of VAPSO-5 and VAPSO-44 indicate the presence of isolated immobile VO^{2+} species of square-pyramidal symmetry, as well as an interaction between the V^{4+} ions which form VO_2 clusters.⁵⁵ This led to the conclusion that vanadium is not capable of occupying tetrahedrally coordinated framework positions in aluminophosphate frameworks.⁵⁵ A cyclic voltammetry study of VAPO-5 also shows that the as-synthesized and calcined samples contain loosely bound VO^{2+} species that can be extracted from the framework.⁵⁶

The coordination and the oxidation number of vanadium sites in VAPO-5 following a redox treatment were investigated by XANES/EXAFS.⁵⁷ On the basis of the spectroscopic and catalytic results, the presence of a framework V^{4+}/V^{5+} redox center is assumed. The following scheme for the oxidation and reduction of vanadium sites has been proposed.⁵⁷



Vanadium incorporation in VAPO-5, -11, -17 and -31 was investigated by UV-Vis, XPS, NMR and ESR techniques.^{58,59} It has been suggested that in calcined VAPOs, isolated tetrahedral V^{5+} is present in the framework positions, substituting for phosphorus. Extra framework isolated and/or polymeric vanadium in square-pyramidal coordination is also present, and these vanadium species can be washed out with an ammonium acetate solution.

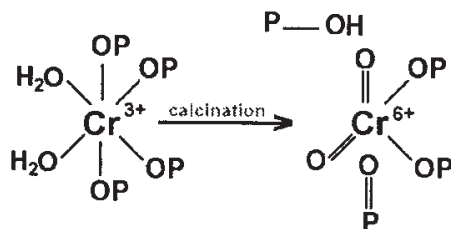
3.3. Chromium

It is well known that Cr(III) ions strongly prefer octahedral coordination. This is evidenced by the scarcity of tetrahedral Cr(III) complexes. Therefore, the incorporation of Cr(III) into an aluminophosphate framework and its substitution for

tetrahedrally coordinated aluminum (or and phosphorus) is rather questionable. Hitherto, there have been controversial opinions about the location of the Cr(III) species.

Structure determination from a small crystal of CrAPO-14 shows that the Cr(III) ions occupy framework sites in the parent AlPO_4 -14 framework. The chromium(III) substitutes for 4–5 % of the aluminum in six-coordinated sites.⁶⁰ However, studies of the DRS spectra and an investigation of the catalytic activity of chromium-containing SAPO-34 in the dehydration of methanol suggest that Cr(III) is not incorporated in the SAPO-34 lattice.⁶¹ The DRS spectrum of the as-synthesized material displays three absorption maxima at 420, 575 and 666 nm, corresponding to $[\text{Cr}(\text{H}_2\text{O})_6]^{3+}$ ions. Upon calcination, the green colour of the material turns to yellow and the spectrum shows only one maximum at 370 nm belonging to CrO_4^{2-} ions. The formation of the chromate ion can be taken as unambiguous evidence for extra-framework Cr(III). Moreover, during the temperature programmed desorption (TPD) of methanol from SAPO and MAPSO (M – Mn, Co, Cr), the MnAPSO and CoAPSO materials exhibit significantly higher desorption temperatures compared to SAPO and the Cr-containing SAPO (SAPO and Cr-containing SAPO show similar desorption temperatures). This is another confirmation that chromium has not built into the SAPO lattice.⁶¹

Isomorphous substitution of Cr(III) into framework sites of AlPO_4 -5 was evidenced by several methods.^{62,63} The distorted octahedral coordination geometry of Cr(III) is suggested to consist of four framework oxygen atoms and two water molecules. It is illustrated by the following scheme:



During calcination, an oxidation of chromium(III) to chromium(VI) occurs leading to the formation of dioxochromium(VI) which is still bonded to the internal aluminophosphate lattice. The acidic P–OH groups derived from the decomposition of the template balance the charges.⁶³

The local environment of the chromium ion in calcined CrAPSO-11 and Cr-SAPO-11 (Cr-exchanged SAPO) was investigated by ESR.⁶⁴ Both solids contain Cr(V). The calcined, hydrated CrAPSO-11 contains square-pyramidally coordinated Cr(V), which gradually converts to Cr(V) in distorted tetrahedral coordination upon dehydration by heating in vacuum. The ESR spectrum of Cr-SAPO-11 also shows the presence of Cr(V), but this species does not convert to tetrahedral coordination upon heating in vacuum. Reduction by hydrogen shows that Cr(V) in Cr-SAPO-11 can be

reduced to species showing a several hundred gauss broad ESR signal, assignable to Cr(III). Reduction by H₂ of calcined CrAPSO-11 does not produce Cr(III) observable by ESR. The ³¹P electron spin echo modulation of CrAPSO-11 shows that Cr(V) is surrounded by about 11–12 phosphorus nuclei at 0.58 nm, which is consistent with Cr(V) in CrAPSO-11 being in a framework phosphorus position.⁶⁴

3.4. Manganese

The incorporation of Mn²⁺ ions into different aluminophosphate frameworks has been reported. There is no doubt that at least a part of the Mn²⁺ ions occupy tetrahedral framework sites. According to the ligand field theory, this is not unexpected since Mn²⁺ (d⁵) does not show any coordination preference.

The location and coordination geometry of Mn(II) in MnAPSO-34 was investigated by diffuse reflectance spectroscopy.⁶¹ The spectrum of the as-synthesized MnAPSO-34 shows several weak absorption maxima. Their positions are essentially in accord with a tetrahedral environment around Mn(II), although it should be pointed out that, in general, the electronic spectra of Mn(II) cannot make a very clear-cut distinction between tetrahedral and octahedral coordination geometries. Upon calcination in air, the colour of MnAPSO-34 changes into violet; when the

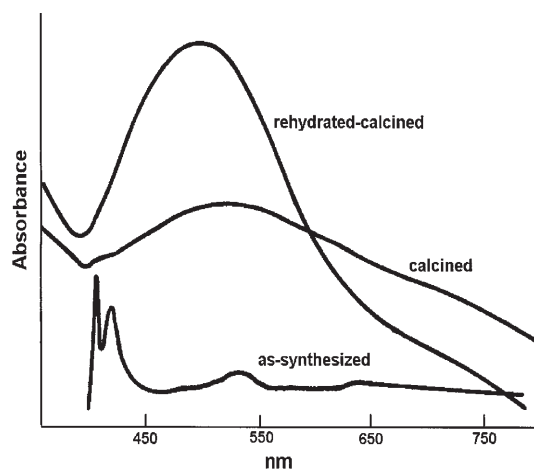


Fig. 4. Diffuse reflectance spectra of MnAPSO-34.

calcined material is then allowed to rehydrate, it turns to reddish. These colour changes are accompanied by changes in the DRS spectra (Fig. 4). Analysis of the spectra shows that calcination of MnAPSO-34 is accompanied by the oxidation of Mn(II) to Mn(III). This is supported by the fact that a subsequent treatment of the calcined material in a stream of hydrogen at 600 °C yields a product that exhibits an identical DRS spectrum to that of the original material. Upon rehydration of calcined MnAPSO-34, the tetrahedral Mn(III) increases its coordination number to 6 through the additional coordination of H₂O molecules.

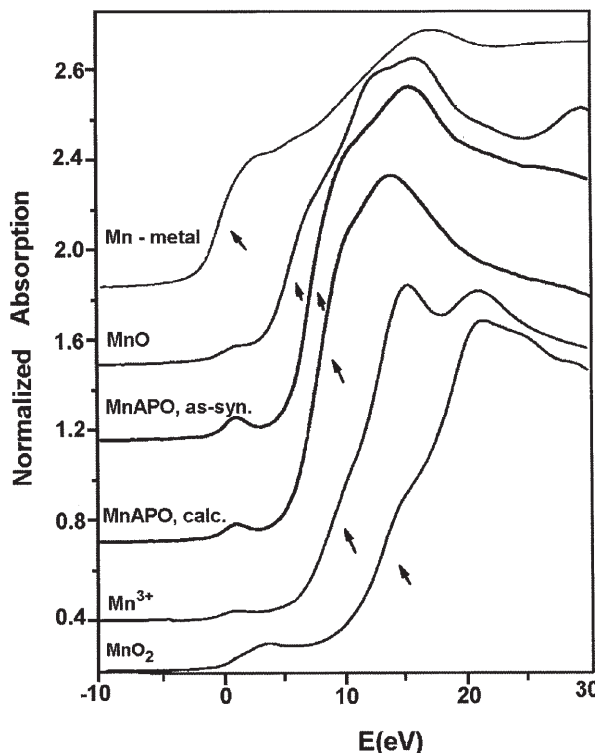


Fig. 5. Normalized Mn K-edge profiles for MnAPO and reference samples. Position of the Mn K-edge is labeled by arrows. Energy scale is given relative to the Mn K-edge of the metal (6539.0 eV).

Octahedral coordination of Mn(III) ions in the rehydrated-calcined MnAPO-34 is also supported by TGA-DTA-DSC analyses.³⁶ Similar results were obtained by Mn K-edge XANES and EXAFS.⁶⁵ A single pre-edge peak is seen in both the as-synthesized and the rehydrated-calcined MnAPO-34 (Fig. 5), indicating that Mn atoms occupy sites without a center of inversion (such as tetrahedral ones). As an example, two resonances are found for the transition metal atoms located at octahedrally coordinated sites (having a center of inversion). EXAFS analysis of MnAPO-34 confirms Mn incorporation into the AlPO_4 -34 framework (Fig. 6). There are four oxygen atoms at 2.02 Å in the first coordination shell of the Mn atom in as-synthesized MnAPO-34. In the rehydrated-calcined sample, four oxygens are found at 2.10 Å and two at the larger distance of 2.37 Å, indicating a distorted octahedral geometry around the Mn(II) ions.

A cluster-like arrangement of Mn^{2+} (Mn-O-P-O-Mn) is found for MnAPO- and MnAPSO-44.⁴⁰ The IR spectra of MnAPO and MnAPSO samples give evidence for P-OH groups (band at 3673 cm^{-1} and a broad band at $3000\text{--}3600\text{ cm}^{-1}$) confirming the framework site of Mn. An adsorption experiment with CD_3CN results in a strong band at 2296 cm^{-1} in the IR spectrum due to a Lewis complex with Mn^{2+} ions.⁴⁰ Similar results on manganese framework site have been obtained by FTIR spectroscopic studies of CO adsorption.⁶⁶

The redox ability of the framework Mn(II) has been found to be a key factor

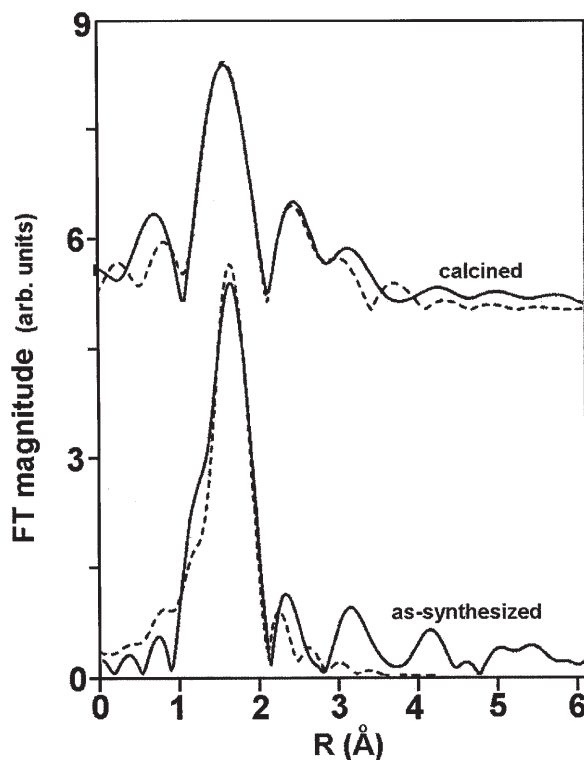


Fig. 6. Fourier transform k^3 weighted EXAFS spectra of as-synthesized and rehydrated-calcined MnAPO-34 calculated in the k range of $4.5\text{--}12 \text{ \AA}^{-1}$ and $4.5\text{--}10 \text{ \AA}^{-1}$, respectively. Solid lines show experimental data whereas dotted lines represent the fitted ones.

for the catalytic activity of MnAPO-5 and MnAPO-18 in the liquid-phase oxidation of cyclohexane by O_2 .⁶⁷

The formation rates of cyclohexanol and cyclohexanone increased linearly with the number of redox-active sites, suggesting that the elementary steps of cyclohexane oxidation involve a cycling between Mn(II) and Mn(III), and require cation sites able to reversibly form charge-balancing cationic species.⁶⁷

The catalytic activity of MnAPO molecular sieves has been a stimulus for the investigation of open-framework manganese phosphates.⁶⁸ Several amines were investigated as possible structure-directing agents. However, they did not exhibit a templating role in the formation of manganese phosphate frameworks. A layer structure was only obtained with 1,2-diaminoethane, which is intercalated between manganese phosphate layers.

3.5. Iron

Incorporation of iron into different aluminophosphate frameworks has been typically investigated using UV-Vis DRS, EPR, IR, Mössbauer and NMR spectroscopies. Although Messina *et al.* in the first report on FAPO-5 supposed (based on chemical analysis) that the substitution of Fe^{3+} and/or Fe^{2+} for both Al^{3+} and P^{5+} occurs,⁶⁹ it is now thought that Fe exclusively substitutes for Al. In the as-synthe-

sized materials, the coexistence of Fe^{3+} and/or Fe^{2+} is mostly found regardless of the iron salt employed (*vide infra*).

Iron is an element exhibiting a Mössbauer effect. Mössbauer spectra of as-synthesized FAPO-5 obtained using either Fe(II) or Fe(III) as the source of iron show the presence of both Fe^{3+} and Fe^{2+} ions (Fe^{3+} : I.S. ≈ 0.3 , Q.S. $\approx 0.8 \text{ mm s}^{-1}$; Fe^{2+} : I.S. ≈ 1.1 , Q.S. $\approx 2.0 \text{ mm s}^{-1}$). The presence of the Fe(II) species in the products obtained using Fe(III) is explained by the following reduction of the Fe(III) by the amine template:



The presence of Fe(III) in the FAPO-5 obtained from the Fe(II) source is explained by aerial oxidation at the gel stage. The oxidation can be minimized using a nitrogen purge.⁷⁰ The presence of Fe(II) and Fe(III) on tetrahedral Al framework sites has also been confirmed by XANES in EXAFS in the large pore FAPO-36⁷¹ and in FAPO-*n* (*n* = 5, 18), by a combination of several techniques.⁷² A computational study of the substitution of Al by Fe^{3+} in AlPO_4 -5 shows that the substitution is energetically unfavourable.⁷³

Iron-substituted aluminophosphate molecular sieves show catalytic activity in the pinacol rearrangement reaction.⁷⁴ It has also been found that FAPO-5 is an exceptionally good catalyst for the selective oxidation of cyclohexane in air.⁷⁵ The catalytic activity is attributed to the redox ability of Fe(III) as an integral part of the APO framework.

Moreover, the open-framework structure coupled with magnetic properties opens the way to a new class of porous materials – magnetic sieves.⁷⁶ For this reason open-framework iron phosphates have attracted great attention in the last few years.^{77–79}

3.6. Cobalt

Cobalt-substituted aluminophosphates are the most extensively investigated MAPO-*n* systems. In comparison to the other first row transition metals, which usually prefer octahedral coordination geometry, Co^{2+} ions adopt rather easily tetrahedral stereochemistry with oxide ions as ligands. This can be explained by the fact that the ligand field stabilization energies for Co^{2+} (ions d^7) disfavour tetrahedral coordination relative to the octahedral one to a lesser extent than is the case for most other d^n configurations. The characteristic royal blue colour of the synthesized CoAPO products is a good indication that cobalt incorporation into the aluminophosphate framework had been achieved.

Single crystal structure analysis of CoAPSO-34 confirms the incorporation of Co^{2+} ions into tetrahedral sites of the chabazite-like framework.⁸⁰ Incorporation of Co(II) ions in the framework of APO- and SAPO-20 leads to an expansion of the parent aluminophosphate unit cell.⁸¹ An analysis of the bond lengths indicates that

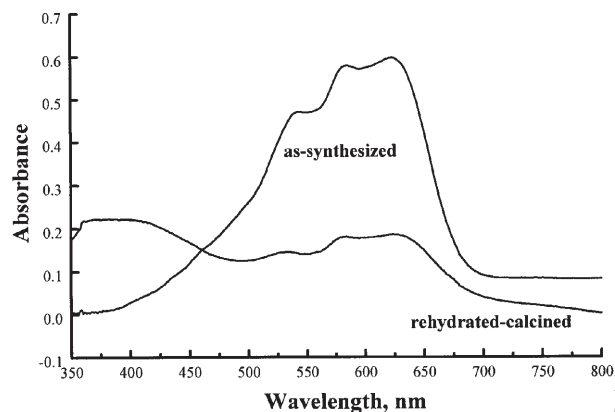
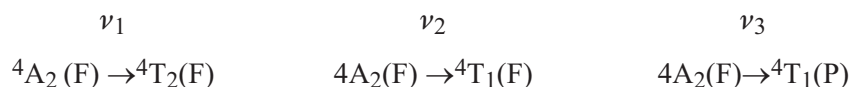


Fig. 7. Diffuse reflectance spectra of CoAPO-34.

the Co distribution over the Al sites is not completely random. The crystal structures of CoAPO-44, CoAPSO-44, CoAPO-47 and CoAPSO-47 were also determined from single crystal X-ray data.⁸² It is suggested that the upper limit to the amount of cobalt (as well as silicon) incorporated and the resulting maximum negative framework charge may be limited by the number of positively charged species, which can fit within the available void space.⁸² Only two template cations (protonated cyclohexylamine) can be packed inside each chabazite cage. The single crystal structure analysis of CoAPO-21 reveals that the Co^{2+} ions occupy exclusively tetrahedral Al-sites, leaving the 5- and 6-coordinated ones intact.⁸³

Diffuse reflectance UV-Vis spectroscopy has been a widely applied method in the investigation of the local geometry of cobalt ions in CoAPO materials. On the basis of a systematic study of the incorporation of Co^{2+} into $\text{AlPO}_4\text{-5}$, a spectroscopic criterion to distinguish between framework and extra-framework Co^{2+} was developed.^{84, 85}

The UV-vis spectrum of a representative CoAPO-34 (Fig. 7) shows a strong absorption in the 500–650 nm region consisting of three components with maxima at 540 (ν_1), 585 (ν_2) and 626 (ν_3) nm. The maxima originate from the following electronic transitions of tetrahedrally coordinated Co(II).



It was also observed that calcination and rehydration induce changes in the spectrum. The spectra of calcined-rehydrated CoAPOs show a considerable decrease in the absorption bands at 500–600 nm and a new strong band at ≈ 370 nm. The assignment of the latter is still controversial. Namely, the change in the spectrum of calcined CoAPO has been attributed either to oxidation of Co^{2+} to Co^{3+} ^{86–88} or to a distortion-induced charge transfer effect without oxidation of the divalent cobalt ions.^{89–91} The controversy about the oxidation of Co^{2+} to Co^{3+} during calcination

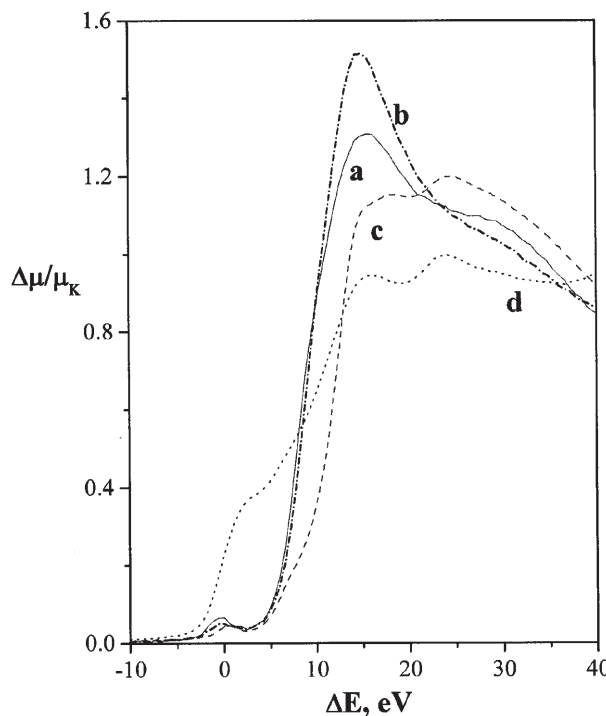


Fig. 8. Normalized Co K-edge profile of as-synthesized (a), calcined-rehydrated CoAPO(b) and the standards: $[\text{Co}(\text{1,2-diaminoethane})_3]\text{Cl}_3$ (c), and Co metal (d).

exists also in the interpretation of ESR spectra in which a significant decrease of the signal occurs after calcination.^{90,91}

The Co K-edge XANES studies of CoAPO-34 performed on as-synthesized and calcined-rehydrated samples indicate a partial oxidation of Co(II) to Co(III) upon calcination (Fig. 8). The Co K-edge of the calcined-rehydrated CoAPO is shifted to a higher energy showing an increase in the Co oxidation number.⁹²

A spin-echo mapping technique has been used to investigate various CoAPO-*n*.⁹³ The different NMR lines of the spectra are assigned to various P(*n*Co) environments in the structure, and their shift is found to be approximately proportional to the number (*n*) of the Co atoms in the first coordination sphere of the P atoms. Also, the presence of signals above 500 ppm is taken as a direct proof for cobalt sitting in the framework.

The incorporation of cobalt has been successful in a number of aluminophosphate structures. However, the substitution level reached is still limited. There are only a few CoAPO-*n* materials (*n* = 44, 46 and 50) with a Co/Al mole ratio greater than 0.3. Recently, a high $\text{Co}^{2+}/\text{Co}^{3+}$ substitution level was obtained in CoAPO-34 and CoAPO-20 using piperidine as the template in a fluoride medium.⁹⁴ Stucky *et al.* have recently developed a new methodology for the preparation of various CoAPO materials with a high percentage of framework Co(II).⁹⁵

Recently, it has been reported that CoAPO-18 could be a good catalyst for the selective oxidation of linear alkanes by molecular oxygen.⁹⁶ Although the precise mechanism of the oxidation is not clear, it is certain that oxidation of the framework Co(II) to Co(III) is vital for the catalysis. A significant factor in facilitating the reaction is also the ability of Co(III) to expand its coordination sphere. MgAPO-18 is totally inactive as an oxidative catalyst since the divalent ion cannot be raised to a higher oxidation state.

3.7. Nickel

Nickel is a good candidate for isomorphous substitution into microporous aluminophosphates because of its versatile coordination chemistry, as well as its catalytic properties. NiAPO-21 was the first reported nickel-substituted aluminophosphate system.⁹⁷ UV/Vis spectroscopy suggests that Ni(II) ions replace the hexacoordinated aluminum of the AlPO_4 -21 framework. The anomalous dispersion technique confirmed the octahedral coordination geometry of the Ni(II).^{98, 99} This method has been used in recent years following the advent of intense tunable X-radiation from synchrotron X-ray sources. By tuning the wavelength of the radiation to be close to the absorption edges of the specific elements, it is possible to identify and distinguish between atoms, which occupy a single site. Thus, by studying the location of Ni in NiAPO-21 by this method, it is found that the Ni atoms fully occupy the octahedral framework sites, forming links between the aluminophosphate layers. Two bonds in the Ni(II) coordination sphere belong to framework O atoms, while the remaining coordination is affected by two 1,2-diaminoethane (which was used as the template), one being monodentate and the other bidentate.⁹⁸

Kevan *et al.* investigated the framework substitution and the local environment of nickel ions in several NiAPSO-*n* molecular sieves ($n = 5, 11, 34, 41$)^{100–103} by ESR and ESEM spectroscopy. In all the systems, the Ni(II) ions are incorporated into the framework positions and various Ni(I) species are formed by reduction and adsorbate interaction. ³¹P ESEM studies of NiAPO-5 indicate that the metal ion incorporation occurs at phosphorous sites.¹⁰⁴

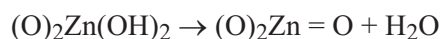
The incorporation of Ni(II) into the framework sites of SAPO-*n* ($n = 17, 18, 34, 35$) affects the catalytic activity of the SAPO materials in the conversion of methanol to olefins. The incorporation of Ni into the structures generally increases the ethene yield. Among the NiAPSO-*n*, NiAPSO-34 shows the best performance in terms of both selectivity and lifetime.¹⁰⁵

3.8. Zinc

Zinc(II) ions adopt equally both the tetrahedral and octahedral coordination geometry with oxide ions as ligands. It could be therefore expected that the incorporation of zinc ions into an aluminophosphate framework should proceed easily.

In the sodalite-like framework (ZnAPO- and ZnAPSO-20), Zn^{2+} ions were found in both the framework and extra-framework positions.⁸¹

The location of Zn(II) ions in AlPO_4 -34 investigated by EXAFS, NMR spectroscopy and the Rietveld X-ray refinement showed that the Zn(II) ions are tetrahedrally coordinated at the positions of Al^{3+} .^{106–108} The ^{31}P -NMR spectrum of ZnAPO-34 exhibits two major signals at -30 and -20 ppm, which are assigned to P(4Al) and P(2Al, 2Zn).¹⁰⁷ The analysis of EXAFS spectra reveals the tetrahedral coordination around Zn(II) with a Zn–O distance of 1.940 \AA . However, the spectrum of calcined ZnAPO shows a decrease in the number of neighbouring O atoms (from four to three), as well as an increase in the Zn–O distance (1.692 \AA). The removal of one oxygen atom upon calcination is explained by the following scheme:



Accordingly, the results of the EXAFS analysis of calcined ZnAPO-34 indirectly confirm the presence of Lewis acid sites as local defect sites in the aluminophosphate lattice.¹⁰⁶ However, the EXAFS analysis of calcined ZnAPO-18 suggests that in this type of structure there are three short and one long bond associated with the Zn–O of the Brønsted acid center.¹⁰⁹

The presence of Brønsted acid sites resulting from Zn(II) incorporation was established on the basis of FTIR analysis of ZnAPO-40.¹¹⁰ The spectrum of ZnAPO-40 shows characteristic peaks at 3610 , 3589 and 3514 cm^{-1} .

Catalytic transformations of 1-butene were performed over ZnAPSO-11 and Zn-supported SAPO-11 (Zn-SAPO).¹¹¹ The ZnAPSO-11 shows a higher selectivity towards skeletal isomerization than Zn-SAPO, which is assigned to the substitution of Al by Zn(II) ions. It is suggested that the substitution leads to the presence of partially coordinatively unsaturated Zn(II) ions in the vicinity of structural P–OH groups. The Brønsted acidity is enhanced by a Brønsted–Lewis interaction, thus rendering the ZnAPO-11 more strongly acidic, a necessity for skeletal isomerization.

The readiness of Zn^{2+} ions to form building blocks suitable for interconnection inside open-framework topologies has had as a result a proliferation of novel open-framework zinc phosphate structures.^{112–117} Among them are even zeolite topologies, such as the sodalite- and faujasite-like. Most of the zincophosphates are novel open-frameworks, such as a chiral zincophosphate, which has been included in the Atlas of Zeolite Framework Types having the structure code CZP.¹¹⁸

4. CONCLUSION

It is evident that open-framework aluminophosphates are characterized by an enhanced structural diversity. The structures differ in topology, pore size and geometry, chemical compositions and the channel dimensionality. These differences in characteristics allow for the "tailoring" of structure and properties. The large family of molecular sieves has been expanded yet again by unique hybrid or-

ganic-inorganic open-frameworks. Both organic and inorganic moieties build up the lattice,^{119,120} which raises the possibility of tuning the dimensions of the pores through the selection of proper organic building blocks.

Among the structures which are zeolite analogues, there are several (such as the chabazite-like $AlPO_4-34$ having a pore opening of about 0.4 nm) which exhibit lattice flexibility rather unusual for the rigid aluminosilicate framework. The degree of structural specificity found in aluminophosphates recommends them for the preparation of novel materials, such as chemical sensors, data storage materials or materials for application in the synthesis of chiral compounds. Finally, open-framework aluminophosphates possess crystallographically ordered nanopores – apertures, cages and channels, the diameters of which are in the range 0.4 to about 1.5 nm. In this respect, open-framework aluminophosphates are good candidates for a new category of catalysts – nanocatalysts. Finally, the porous aluminophosphate lattice could be a promising host for the preparation of nano materials. Very recently, a silica matrix was successfully used for the preparation of nano ferrites.¹²¹

ИЗВОД

ПОРОЗНИ АЛУМОФОСФАТИ: СИНТЕЗА, КАРАКТЕРИЗАЦИЈА И
МОДИФИКОВАЊЕ ЈОНИМА ПРЕЛАЗНИХ МЕТАЛА

НЕВЕНКА РАЈИЋ

Технолошко-металуришки факултет, Карнегијева 4, 11000 Београд

Кратак ревијални приказ порозних алумофосфата и њихових модификација које садрже јоне прелазних метала. За ове материјале је карактеристична структурна и хемијска разноликост, као и различите димензије пора које су уређене у кристалографском смислу и чија величина се може подешавати променом услова синтезе. Пречник пора, кавеза и канала је у опсегу од 0,4 до 1,5 nm што алумофосфате чини применљивим у области нано-катализе. Уграђивањем јона прелазних метала са редокс својствима у решетки алумофосфата настају активни центри чиме алумофосфати постају применљиви и као селективни би-функционални катализатори. Да би се стекао увид у положај и координациону геометрију јона прелазних метала, морају се користити различите инструменталне технике.

(Примљено 11. новембра 2004)

REFERENCES

1. S. T. Wilson, B. M. Lok, E. M. Flanigen, U. S. Patent, 4,310,440 (1982)
2. S. T. Wilson, B. M. Lok, C. A. Messina, T. R. Cannan, E. M. Flanigen, *J. Am. Chem. Soc.* **104** (1982) 1146
3. *Atlas of Zeolite Framework Types*, Ch. Baerlocher, W. W. Meier, D. H. Olson, Eds., Fifth Revised Ed., Elsevier, Amsterdam, 2001
4. B. M. Lok, C. A. Messina, R. L. Patton, R. T. Gajek, T. R. Cannan, E. M. Flanigen, U. S. Patent 4,440,871 (1984)
5. B. M. Lok, C. A. Messina, R. L. Patton, R. T. Gajek, T. R. Cannon, E. M. Flanigen, *J. Am. Chem. Soc.* **106** (1984) 6092
6. C. A. Messina, B. M. Lok, E. M. Flanigen, U. S. Patent 4,544,143 (1985)

7. S. T. Wilson, E. M. Flanigen, U. S. Patent 4,567,029 (1986)
8. R. L. Patton, S. T. Wilson, E. M. Flanigen, European Patent 158,349 (1985)
9. B. M. Lok, B. K. Marcus, E. M. Flanigen, European Patent 158,350 (1985)
10. B. M. Lok, B. K. Marcus, E. M. Flanigen, European Patent 161,490 (1985)
11. B. M. Lok, D. L. Vail, E. M. Flanigen, European Patent 158,975 (1985)
12. B. M. Lok, B. K. Marcus, E. M. Flanigen, European Patent 161,489 (1985)
13. N. Rajić, R. Gabrovšek, V. Kaučič, *Thermochim. Acta* **359** (2000) 119
14. N. Rajić, V. Kaučič, D. Stojaković, *Zeolites* **10** (1990) 169
15. J. B. M. Weckhuysen, D. Baetens, R. Schoonheydt, *Angew. Chem. Int. Ed.* **39** (2000) 3419
16. A. N. Christensen, P. Norby, C. J. Hanson, *Acta Chem. Scand.* **51** (1997) 249
17. P. Norby, C. J. Hanson, *Catal. Today* **39** (1998) 301
18. S. Oliver, A. Kuperman, G. A. Ozin, *Angew. Chem. Int. Ed.* **37** (1998) 46
19. K. Wang, J. Yu, R. Xu, *Inorg. Chem.* **42** (2003) 4597
20. J. Batista, V. Kaučič, N. Rajić, D. Stojaković, *Zeolites* **12** (1992) 925
21. C. N. R. Rao, *Indian J. Chem.* **42** (2003) 2163
22. N. Rajić, N. Zabukovec Logar, S. Sajić, D. Stojaković, V. Kaučič, *J. Serb. Chem. Soc.* (2004), to be published
23. N. J. Tapp, N. B. Milestone, D. M. Bibby, *Zeolites* **8** (1988) 183
24. A. F. Ojo, L. B. McCusker, *Zeolites* **11** (1991) 460
25. A. K. Sinha, S. Sainkar, S. Sivasanker, *Micropor. Mesopor. Mater.* **31** (1999) 321
26. K. J. Balkus, Jr., A. G. Gabrielov, S. Shepelev, *Microporous Mater.* **3** (1995) 489
27. K. J. Balkus, Jr., A. G. Gabrielov, N. Sandler, *J. Porous Mater.* **1** (1995) 199
28. N. Rajić, A. Meden, P. Sarv, V. Kaučič, *Micropor. Mesopor. Mat.* **24** (1998) 83
29. A. Meden, L. B. McCusker, C. Baerlocher, N. Rajić, V. Kaučič, *Micropor. Mesopor. Mat.* **47** (2001) 260
30. N. Rajić, D. Stojaković, V. Kaučič, in *Proceedings of the 12th International Zeolite Conference*, M. M. J. Treacy, B. K. Marcus, M. E. Bisher, J. B. Higgins, Eds., MRS, Warrendale, 1999, p. 1765
31. N. Rajić, N. Zabukovec Logar, A. Golubić, V. Kaučič, *J. Phys. Chem. Solids* **64** (2003) 1097
32. N. Rajić, D. Stojaković, V. Kaučič, *Zeolites* **10** (1990) 802
33. N. Rajić, D. Stojaković, N. Novak Tusar, *ACH-Models Chem.* **135** (1998) 101
34. R. Jelinek, B. F. Chmelka, Y. Wu, P. J. Grandinetti, A. Pines, P. J. Barrie, J. Klinowski, *J. Am. Chem. Soc.* **113** (1991) 4097
35. J. W. Richardson, Jr., J. V. Smith, J. J. Pluth, *J. Phys. Chem.* **93** (1989) 8212
36. N. Rajić, R. Gabrovšek, A. Ristić, V. Kaučič, *Thermochim. Acta* **306** (1997) 31
37. A. Tuel, S. Caldarelli, A. Meden, L. B. McCusker, Ch. Baerlocher, A. Ristić, N. Rajić, G. Mali, V. Kaučič, *J. Phys. Chem.* **104** (2000) 5697
38. H. Kessler, in *Synthesis, Characterization and Novel Applications of Molecular Sieves Materials (Mat. Res. Soc. Symp. Proc., Vol. 233)*, R. L. Bedard, et al. (Eds.), MRS, Pittsburgh, 1991, p. 47
39. M. E. Davis, C. Montes, P. Hathaway, J. Arhancet, D. L. Hasha, J. Garces, *J. Chem. Soc.* **111** (1989) 3919
40. U. Lohse, A. Bruckner, E. Schreirer, R. Bertam, J. Janchen, R. Fricke, *Microporous Mater.* **7** (1996) 139
41. J. Garcia Carmona, R. Rodriguez Clemente, J. Gomez Morales, *Zeolites* **18** (1997) 340
42. I. Braun, G. Schulz-Ekloff, D. Wohrle, W. Lautenschlager, *Micropor. Mesopor. Mater.* **23** (1998) 79
43. M. Park, S. Komarneni, *Micropor. Mesopor. Mater.* **20** (1998) 39
44. I. Girnus, K. Jancke, R. Vetter, J. Richter-Mendau, J. Caro, *Zeolites* **15** (1995) 33
45. E. M. Flanigen, R. L. Patton, S. T. Wilson, in *Innovation in Zeolite Materials Science (Stud. Surf. Sci. Catal. Vol. 37)*, P. J. Grobet, W. J. Mortier, E. F. Vansant, G. Schulz-Ekloff, Eds., Elsevier, Amsterdam, 1988, p. 13
46. N. Rajić, V. Kaučič, "Molecular sieves: aluminophosphates" in *Encyclopedia of Catalysis*, I. Horvath, T. István, Eds., Wiley-Interscience, New York, 2002/2003, pp. 188–236

47. G. Deo, A. Turek, I. E. Wachs, D. R. C. Huybrechts, P. A. Jacobs, *Zeolites* **13** (1993) 365
48. R. Millini, E. P. Massara, G. Perego, G. Bellussi, *J. Catal.* **137** (1992) 497
49. S. Bordiga, S. Coluccia, C. Lamberti, L. Marchese, A. Zecchina, F. Boscherini, F. Buffa, F. Genoni, G. Leofanti, G. Petrini, G. Vlaic, *J. Phys. Chem.* **98** (1994) 4125
50. A. J. H. P. van der Pol, A. J. Verduyn, J. H. C. van Hooff, *Appl. Catal.* **92** (1992) 113
51. D. R. C. Huybrechts, P. L. Buskens, P. A. Jacobs, *J. Mol. Catal.* **71** (1992) 129
52. A. Tuel, *Zeolites* **15** (1995) 228
53. M. H. Zahedi-Niaki, S. M. Zaidi, S. Kaliaguine, *Micropor. Mesopor. Mater.* **32** (1999) 251
54. N. Venkatathri, S. G. Hegde, S. Sivasanker, *Indian J. Chem. A* **42** (2003) 974
55. U. Lohse, A. Bruckner, K. Kintscher, B. Parltitz, E. Schreier, *J. Chem. Soc. Faraday T.* **91** (1995) 1173
56. F. Bedioui, E. Briot, J. Devynck, K. J. Balkus, Jr., *Inorg. Chem. Acta* **254** (1997) 151
57. K. J. Chao, A. C. Wei, H. C. Wu, J. F. Lee, *Catal. Today* **49** (1999) 277
58. T. Blasco, P. Concepcion, P. Grotz, J. M. Lopez Nieto, A. Martinez-Arias, *J. Mol. Catal. A-Chem.* **162** (2000) 267
59. M. Hassan Zahedi-Niaki, S. M. Javaid Zaidi, S. Kaliaguine, *Appl. Catal. A-Gen.* **196** (2000) 9
60. M. Helliwell, V. Kaučić, G. M. T. Cheetham, M. M. Harding, B. M. Kariuki, P. J. Rizkallah, *Acta Cryst. B* **49** (1993) 413
61. N. Rajić, D. Stojaković, S. Hočevar, V. Kaučić, *Zeolites* **13** (1993) 384
62. J. Kornatowski, G. Zadrozna, in *Proceedings of the 12th International Zeolite Conference*, M. M. J. Treacy, B. K. Marcus, M. E. Bisher, J. B. Higgins, Eds., MRS, Warrendale, 1999, p. 1577
63. J. D. Chen, R. A. Sheldon, *J. Catal.* **153** (1995) 1
64. Z. Zhu, T. Wasowicz, L. Kevan, *J. Phys. Chem. B* **101** (1997) 10763
65. I. Arcon, N. Rajić, A. Kodre, *J. Synchrotron Rad.* **6** (1999) 460
66. N. Novak Tušar, N. Zbukovec Logar, I. Arčon, F. Thibault-Starzyk, A. Ristić, N. Rajić, V. Kaučić, *Chem. Mater.* **15** (2003) 4745
67. B. Moden, L. Oliviero, J. Dakka, J. G. Santiesteban, E. Iglesia, *J. Phys. Chem. B* **108** (2004) 5552
68. N. Rajić, A. Ristić, V. Kaučić, *Zeolites* **17** (1996) 304
69. C. A. Messina, B. M. Lok, E. M. Flanigen, Eur. Pat. Appl., 131,946 (1985)
70. A. F. Ojo, J. Dwyer, R. V. Parish, in *Zeolites: Facts, Figures, Future (Stud. Surf. Sci. Catal., Vol. 49A)*, P. A. Jacobs, R. A. van Santen, Eds., Elsevier Science Publishers B.V., Amsterdam, 1989, p. 227
71. A. Ristić, N. Novak Tušar, I. Arcon, N. Zbukovec Logar, F. Thibault-Starzyk, J. Czyżniewska, V. Kaučić, *Chem. Mater.* **15** (2003) 3643
72. C. Zenonos, G. Sankar, F. Cora, D. W. Lewis, Q. A. Pankhurst, C. R. A. Catlow, J. M. Thomas, *Phys. Chem. Chem. Phys.* **4** (2002) 5421
73. J. G. Gonzalez, J. de la Cruz Alcaz, A. R. Ruiz-Salvador, A. Gomez, A. Dago, C. de las Pozas, *Micropor. Mesopor. Mat.* **29** (1999) 361
74. B.-Y. Hsu, S. Cheng, *Micropor. Mesopor. Mat.* **21** (1998) 505
75. R. Raja, G. Sankar, J. M. Thomas, *J. Am. Chem. Soc.* **121** (1999) 11926
76. M. Riou-Cavellec, D. Riou, G. Ferey, *Inorg. Chim. Acta* **291** (1999) 317
77. U. R. Pillai, E. Sahle-Demessie, *Chem. Commun.* (2004) 826
78. N. Rajić, D. Stojaković, D. Hanzel, N. Zbukovec Logar, V. Kaučić, *Micropor. Mesopor. Mater.* **55** (2002) 313
79. N. Rajić, D. Stojaković, D. Hanzel, V. Kaučić, *J. Serb. Chem. Soc.* **69** (2004) 179
80. G. Nardin, L. Randaccio, V. Kaučić, N. Rajić, *Zeolites* **11** (1991) 192
81. N. Rajić, D. Stojaković, V. Kaučić, *Aust. J. Chem.* **44** (1991) 543
82. J. M. Bennett, B. K. Marcus in *Innovation in Zeolite Materials Science (Stud. Surf. Sci. Catal. Vol. 37)*, P. J. Grobet *et al.* (Eds.), Elsevier Science Publishers B. V., Amsterdam, p. 269
83. G. M. T. Cheetham, M. M. Harding, P. J. Rizallah, V. Kaučić, N. Rajić, *Acta Cryst. C* **47** (1991) 1361
84. A. A. Verberckmoes, M. G. Uytterhoeven, R. A. Schoonheydt, *Zeolites* **19** (1997) 180

85. A. A. Verberckmoes, B. M. Weckhuyen, R. A. Schoonheydt, *Micropor. Mesopor. Mater.* **22** (1998) 165
86. B. W. Weckhuysen, R. R. Rao, J. A. Martens, R. A. Schoonheydt, *Eur. J. Inorg. Chem.* (1999) 565
87. U. Lohse, R. Bertram, K. Jancke, I. Kurzawski, B. Parltitz, E. Löffler, E. Schreier, *J. Chem. Soc. Faraday T.* **91** (1995) 1163
88. S. Thomson, V. Luva, R. Howe, *Phys. Chem. Chem. Phys.* **1** (1999) 615
89. J. Sponer, J. Cejka, J. Dedecek, B. Wichterlova, *Micropor. Mesopor. Mat.* **37** (2000) 117
90. C. Montes M. E. Davis, B. Murray, M. Narayana, *J. Phys. Chem.* **94** (1990) 6425
91. V. Kurshev, L. Kevan, D. J. Parillo, C. Pereira, G. T. Kokotailo, R. J. Gorte, *J. Phys. Chem.* **98** (1994) 10160
92. N. Rajić, I. Arčon, V. Kaučič, A. Kodre, *Croat. Chem. Acta* **72** (1999) 645
93. L. Canesson, Y. Boudeville, A. Tuel, *J. Am. Chem. Soc.* **119** (1997) 10754
94. N. Rajić, R. Gabrovšek, V. Kaučič, *Thermochim. Acta* **351** (2000) 119
95. P. Feng, X. Bu, G. Stucky, *Nature* **388** (1997) 735
96. J. M. Thomas, R. Raja, G. Sankar, R. G. Bell, *Nature* **398** (1999) 227
97. N. Rajić, D. Stojaković, V. Kaučič, *Zeolites* **11** (1991) 612
98. M. Helliwell, B. Gallois, B. M. Kariuki, V. Kaučič, J. R. Helliwell, *Acta Cryst. B* **49** (1993) 420
99. M. Helliwell, *J. Synch. Rad.* **7** (2000) 139
100. M. Hartmann, N. Azuma, L. Kevan, *J. Phys. Chem.* **99** (1995) 10988
101. N. Azuma, C. W. Lee, L. Kevan, *J. Phys. Chem.* **98** (1994) 1217
102. M. Djieugoue, A. M. Prakash, L. Kevan, *J. Phys. Chem. B* **103** (1999) 804
103. A. M. Prakash, M. Hartmann, L. Kevan, *J. Chem. Soc. Faraday T.* **93** (1997) 1233
104. A. M. Prakash, M. Hartmann, Z. D. Zhu, L. Kevan, *J. Phys. Chem. B* **104** (2000) 1610
105. M. Djieugoue, A. M. Prakash, L. Kevan, *J. Phys. Chem. B* **104** (2000) 6452
106. A. Tuel, I. Arcon, N. Tusar, A. Meden, V. Kaučič, *Microporous Mater.* **7** (1996) 271
107. N. Tušar, V. Kaučič, S. Geremia, G. Vlaić, *Zeolites* **15** (1995) 708
108. G. Gonzales, C. Pina, A. Jacas, M. Hernandez, A. Leyva, *Micropor. Mesopor. Mater.* **25** (1998) 103
109. G. Sankar, J. M. Thomas, J. Chen, P. A. Wright, P. A. Barrett, G. N. Greaves, C. R. A. Catlow, *Nuclear Instruments & Methods in Physics Research Section B – Beam Interactions with Materials and Atoms* **97** (1995) 37
110. J. P. Lourenco, M. F. Ribeiro, C. Borges, J. Rocha, B. Onida, E. Garrone, Z. Gabelica, *Micropor. Mesopor. Mater.* **38** (2000) 267
111. D. Escalante, B. Mendez, G. Hernandez, C. M. Lopez, F. J. Machado, J. Goldwasser, M. M. R. de Agudelo, *Catal. Lett.* **47** (1997) 229
112. S. Mandal, S. Natarajan, *Inorg. Chim. Acta* **357** (2004) 1437
113. Z. E. Lin, Q. X. Zhang, B. Y. Yang, *Micropor. Mesopor. Mater.* **64** (2003) 119
114. N. Zabukovec Logar, N. Rajić, V. Kaučič, L. Golič, *J. Chem. Soc. Chem. Commun.* (1995) 1681
115. N. Rajić, N. Zabukovec Logar, V. Kaučič, *Zeolites* **15** (1995) 672
116. N. Rajić, R. Gabrovšek, V. Kaučič, *Thermochim. Acta* **278** (1996) 157
117. N. Rajić, N. Zabukovec Logar, A. Meden, V. Kaučič, in *Synthesis of Porous Materials: Zeolites, Clays, and Nanostructures*, M. Occelli, H. Kessler, Eds., Marcel Dekker, New York, 1997
118. <http://www.iza-structure.org/databases/>
119. G. Mali, N. Rajić, N. Zabukovec Logar, V. Kaučič, *J. Phys. Chem.* **B 107** (2003) 1286
120. N. Rajić, N. Zabukovec Logar, G. Mali, V. Kaučič, *Chem. Mater.* **15** (2003) 1734
121. N. Rajić, M. Čeh, R. Gabrovšek, V. Kaučič, *J. Am. Ceram. Soc.* **85** (2002) 1719.